Mechanisms of Development 123 (2006) 881–892

www.elsevier.com/locate/modo

Xenopus cadherin-6 regulates growth and epithelial development of the retina

Gui Ruan, Doris Wedlich, Almut Koehler *

University of Karlsruhe (TH), Institute of Zoology II, Karlsruhe, Germany

Received 5 April 2006; received in revised form 21 August 2006; accepted 27 August 2006
Available online 1 September 2006

Abstract

Cadherins are crucial for tissue cohesion, separation of cell layers and cell migration during embryogenesis. To investigate the role of classical type II Xcadherin-6 (Xcad-6), we performed loss-of-function studies by morpholino oligonucleotide injections. This resulted in severe eye defects which could be rescued with murine cadherin-6. In the absence of Xcadherin-6, morphological alterations and a decrease in cell proliferation were observed with eye cup formation. Eye field transplantations of Xcadherin-6 depleted donors yielded grafts that failed to form a proper neuroepithelium in a wildtype environment. At later developmental stages Xcadherin-6 deficient eyes showed lamination defects in the outer neural retina, a reduced thickness of the ganglion cell layer (GCL) and a fragmented retina pigment epithelium (RPE). Thus, Xcadherin-6 is essential early in eye development for structural organization and growth of the neuroepithelium before it differentiates into neural retina and RPE.

Keywords: Cadherins; *Xenopus*; Retina; Eye; Organization; Cadherin-6

1. Introduction

Cadherins form a superfamily of transmembrane cell-cell adhesion molecules. Although the extracellular part of each type of cadherin has common features with other family members, it is specific in mediating homophilic binding between cadherins of the same type (Shapiro et al., 1995; Takeichi, 1995; Angst et al., 2001). Initially, cadherins were identified in epithelia required for cell polarity and for establishing tissue integrity (Hatta and Takeichi, 1986; Matsunaga et al., 1988; McNeill et al., 1990; see also reviews Nelson et al., 1990; Kemler, 1992). The cadherin superfamily is subdivided in the subfamilies classical cadherins, fat cadherins, protocadherins, flamingo cadherins and others according to their different domain structures (Nollet et al., 2000; Yagi and Takeichi, 2000). The classical cadherins share the β-catenin binding site but vary in the extracellular domain structure. Type I and II of the classical cadherins possess five of the conserved tandem repeats (EC domains) which characterize cadherins. They differ in the adhesion tripeptide found within the EC1 domain, while EC2 and the transmembrane domain are highly conserved domains (Shimoyama et al., 2000). More recently, Patel et al. (2006) determined the crystal structure of type II cadherins which shows important differences in the adhesive interfaces of the EC1 domains compared to type I cadherins. Two tryptophan residues instead of a single one found in type I cadherins reach into the hydrophobic pocket of the homophilic partner. In addition the adhesive interface of type II cadherins appears extended compared to that of type I cadherins. These structural differences explain why type I and type II cadherin expressing cells seggregate (Patel et al., 2006) and further address the question about their different roles in organogenesis.

Most cadherins are expressed in the central nervous system. Because each of them displays a unique expression pattern restricted to segment boundaries and brain com-

* Corresponding author. Tel.: +49721 6084196; fax: +49721 6083992.
E-mail address: almut.koehler@zi2.uka.de (A. Koehler).

0925-4773/$ - see front matter
doi:10.1016/j.mod.2006.08.010

partments, Redies and Takeichi (1996) hypothesized that an adhesion code defines brain architecture. Bekirov et al. (2002) further supported this hypothesis, showing that differential but also partially overlapping expression fields of cadherins reflect anatomical boundaries.

As part of the diencephalon the eye develops by extreme morphogenetic movements. First, the prospective eye field in the anterior neural plate is separated into two fields (Woo and Fraser, 1995; Li et al., 1997). Later, an optic vesicle forms, which makes contact with the overlaying surface ectoderm and induces lens development. In parallel with the developing lens, the optic vesicle invaginates, thus forming an optic cup with a two-layered wall. The inner wall further develops to a multilayered neural retina while the outer one keeps its monolayer structure and becomes pigmented to form the non-neural RPE (retinal pigment epithelium). The neural retina thickens and laminates into the ganglion cell layer (GCL), inner plexiform layer (IPL), inner nuclear layer (INL), outer plexiform layer (OPL), and outer nuclear layer (ONL) (Hoar, 1982; Bron et al., 1997). In sum, there are different periods during eye development when cadherins could play a role in cell sorting and cell movement: separation of the eye field, invagination of the optic cup, lamination and differentiation of the neural retina.

Several cadherins (N-cadherin, R-cadherin, cadherin-11, cadherin-2, 4, 6, 7, and 8, P-cadherin, E-cadherin, Hz-cadherin, FAT1 and protocadherin-15b) have been reported to be expressed in the vertebrate eye (Wöhrn et al., 1998; Liu et al., 1999, 2001; Honjo et al., 2000; Xu et al., 2002; Tanabe et al., 2004; Babb et al., 2005; Seiler et al., 2005). Each exhibits a specific expression pattern, and some, e.g., N-cadherin, cadherin-11, and cadherin-8, dynamically change their expression during retina differentiation (Honjo et al., 2000). Cadherin function has been most intensively studied in the zebrafish eye. Corresponding to the individual expression profiles, specific knockdown and mutant phenotypes were observed. R-Cadherin (cdh4) knockdown resulted in smaller eyes due to an increase in apoptosis with strong defects in axon projection (Babb et al., 2005). Zebrafish protocadherin 15b (PCDH15b) knockdown led to clumping of the outer segments of photoreceptor cells (Seiler et al., 2005). Four reports on N-cadherin mutants in zebrafish (Pujic and Malicki, 2001; Erdmann et al., 2003; Masai et al., 2003; Malicki et al., 2003) revealed that this cadherin is required for proper retina lamination, outgrowth of neuronal processes from amacrine cells and pathfinding of ganglion cell axons. Functional studies on cadherin-6 in eye development have not been reported so far. Although cadherin-6 is expressed in the mouse eye (Honjo et al., 2000), eye development was not been considered in the knockout study (Inoue et al., 2001).

To investigate Xcadherin-6 function in eye development, we blocked Xcadherin-6 protein synthesis by antisense morpholino oligonucleotides (Xcad-6MO). Separation of the eye field and formation of the eye vesicles occurred properly; however, during eye cup formation structural defects in the primordia of the neural retina and the RPE were observed. Transplantation assays revealed that grafts injected with Xcad-6MO failed to develop a proper neuroepithelial structure in the presumptive neural retina and RPE. Cell proliferation in the developing eye of Xcadherin-6 depleted embryos was reduced, leading to smaller eyes and lenses. Cell differentiation was not affected, but the lamination of the neural retina was disturbed as photoreceptor cells were found misplaced in the inner nuclear layer. From these data, we conclude that Xcadherin-6 expression in the eye is necessary for structural organization and growth of the neuroepithelium that later gives rise to neural retina and non-neural RPE.

2. Results

2.1. Xcadherin-6 knockdown results in eye defects

We have previously shown by in situ hybridization that Xcadherin-6 is expressed in placodes and in the developing eye (David and Wedlich, 2000). To study the function of Xcadherin-6, we blocked its translation by injection of Xcadherin-6 antisense morpholino oligonucleotide (Xcad-6MO). The morpholino was complementary to a sequence spanning the ATG start codon of the Xcadherin-6 gene (Fig. 1A). A 25 bp morpholino oligonucleotide that, apart from the ATG codon, did not show any similarity with the Xcadherin-6 gene was used as control (CoMO).

The efficiency of the Xcad-6MO to block the translation of the Xcadherin-6 gene was examined by immunoblotting at tadpole stage 31/32. Injection of 8 μM Xcad-6MO completely suppressed endogenous Xcadherin-6 synthesis, whereas similar amounts of CoMO had no effect (Fig. 1B). As loading control we used XE-cadherin, which was detected in all embryo lysates in comparable amounts. The latter demonstrates the specificity of the Xcad-6MO (Fig. 1B). The Xcadherin-6 antibody was produced against 15 amino acids of the first extracellular domain (EC1) of Xcadherin-6. The specificity of this antibody was documented by immunoblotting with in vitro synthesized fusion proteins of Xcadherin-6/GFP, Xcadherin-11/myc and XE-cadherin/myc. While the Xcadherin-6 antibody recognized a 118 kDa protein, which represented the expected size of unglycosylated Xcadherin-6 fused to GFP, no signal was detected for myc tagged Xcadherin-11 and XE-cadherin (Fig. 1C). Antibodies directed against the different tag proteins (GFP or myc, respectively) confirmed that all fusion proteins were successfully synthesized. We further proved the specificity of the antisense morpholino in an in vitro translation assay. In contrast to Xcadherin-6 neither XN-cadherin nor murine cadherin-6 translation was suppressed by Xcad-6MO (Fig. 1D).

Embryos injected with 4 μM Xcadherin-6 morpholino oligonucleotide into one dorsal blastomere at four-cell stage displayed in 65% of individuals eye phenotypes which varied between missing eyes (7%), eyes with abnormal structures and pigmentation defects (30%) and eyes of

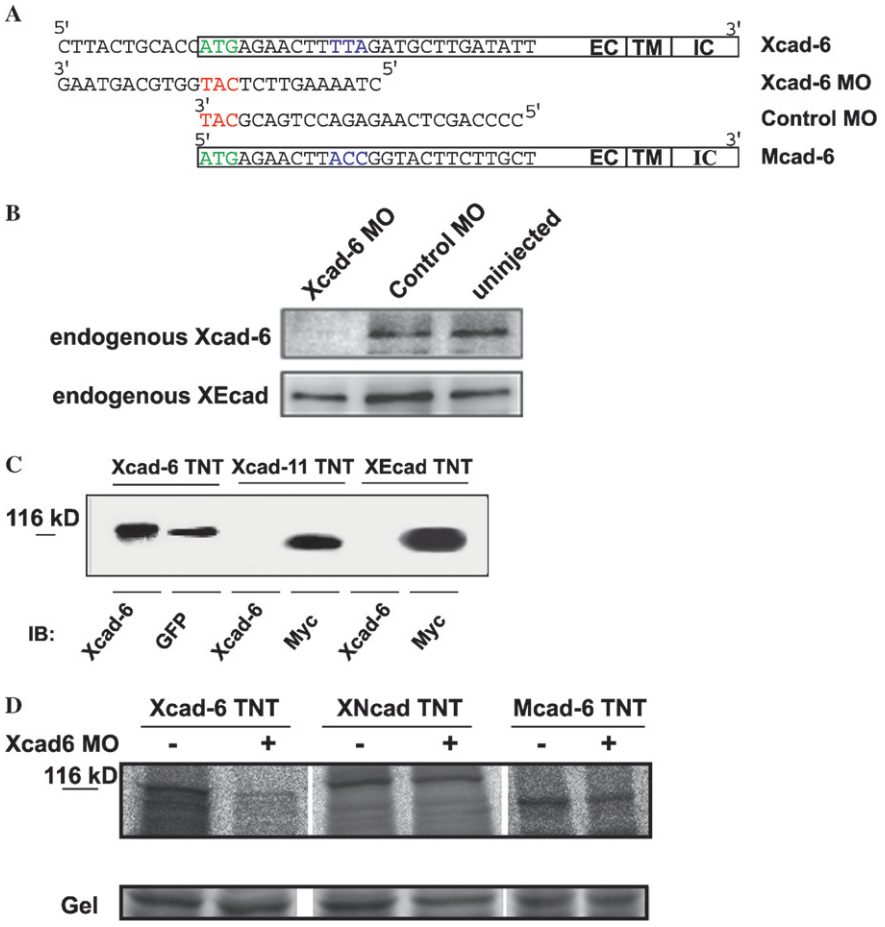

Fig. 1. Xcadherin-6 knockdown. (A) Sequence of antisense (Xcad-6MO) and control (CoMO) morpholino aligned to Xcadherin-6 and the murine homologue (Mcad-6) (B) Immunoblot demonstrating the efficiency of Xcad-6MO in specifically blocking Xcadherin-6 synthesis. No Xcad-6 signal was detected in ConA lysates from stage 31/32 embryos injected with 8 μM Xcad-6MO, whereas Xcadherin-6 was present in lysates from CoMO injected or uninjected control embryos. XE-cadherin was not affected and served as loading control (lower blot). Lysates from uninjected embryos of the same stage act as positive controls. MO, morpholino; CoMO, control morpholino; Mcad-6, murine cad-6; XEcad, *Xenopus* E-cadherin. (C) Immunoblot demonstrating specificity of a Xcadherin-6 antibody directed against the first extracellular domain. In vitro synthesized proteins of Xcad-6/GFP, Xcad-11/myc, and XE-cad/myc were incubated with the corresponding antibodies. The Xcad-6 antibody detects Xcadherin-6, but not Xcadherin-11 or XE-cadherin, whereas anti-GFP or anti-myc antibodies recognize the corresponding fusion proteins. (D) In vitro translation assay showing the repression of Xcad-6 synthesis in presence of 10 μM Xcad-6MO whereas translation of XN-cadherin and murine cadherin-6 was not affected. 1 μg DNA of the corresponding expression plasmid were used in this assay.

smaller size (28%; $n = 284$ embryos) on the injected side of stage 39/40 embryos (Fig. 2A and B). The injected side was traced by expression of co-injected GFP mRNA. Injection of 4 μM control morpholino together with 200 pg GFP mRNA had no influence on the eye phenotype (0.5% abnormal eyes, 4% reduced eyes; $n = 388$ embryos) compared with injections of 200 pg GFP mRNA alone (4% abnormal eyes, 5% reduced eyes; $n = 324$ embryos). To demonstrate the specificity of the Xcad-6MO effect, we sought to rescue the eye phenotype using murine cadherin-6 DNA (Mcad-6). Mcad-6 shares an amino acid sequence identity of 74% with Xcadherin-6 and exhibits a comparable expression pattern. The in vitro translation (Fig. 1D) shows that the three mismatches found in the sequence following the ATG codon are sufficient to prevent a translational block by Xcad-6MO. Co-injection of 100 pg Mcad-6 DNA together with Xcad-6MO and GFP mRNA resulted in a clear rescue of the eye phenotypes (Fig. 2B). Eighty-one percent of the injected embryos showed a normal eye whereas 14.5% of the embryos exhibited a reduced and 4% an abnormal eye phenotype. Only in 0.5% of the embryos no eye was formed on the injected side. The rescue effect was further confirmed in histological sections, which showed no differences in the eye structures between the uninjected and the injected side (Fig. 2C).

2.2. Xcadherin-6 is expressed in the eye field but is not required for eye field separation

Next we investigated at which time point Xcadherin-6 becomes essential in eye development. Because cadherins play important roles in tissue separation, we hypothesized that Xcadherin-6 might be involved in eye field separation, which takes place during stages 13–18. As described earlier,

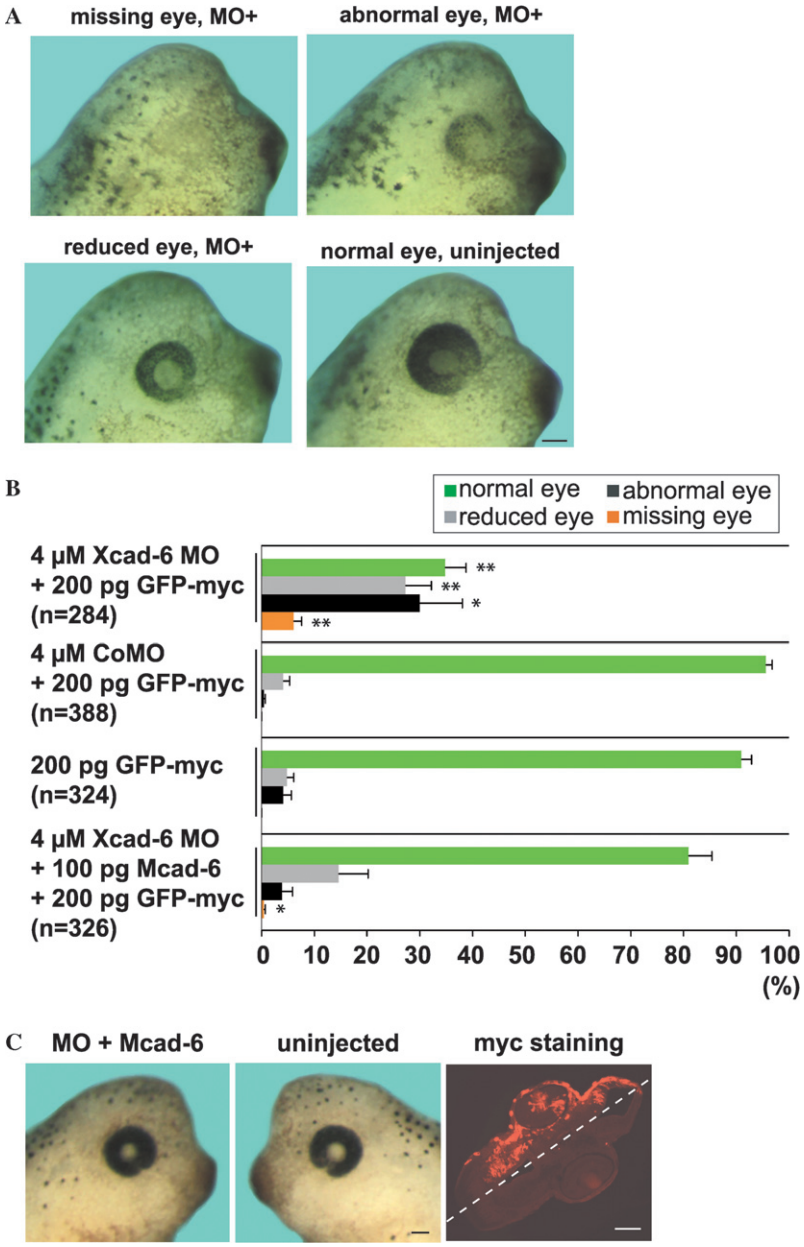

Fig. 2. Xcadherin-6 MO phenotype. (A) Xcad-6MO eye phenotypes classified according to three categories: missing eye, abnormal eye, reduced eye. The sizes of the abnormal eye and the reduced eye phenotype were in the same range covering only 60–80% of the wildtype eye area. The abnormal eye additionally exhibited a pigmentation defect. Only the dorsal part of the eye showed a weak crescent like pigmentation. (B) Statistical evaluation of eye defects as indicated. The Xcadherin-6 knockdown led in 65% of the cases to embryos with eye defects; these could be rescued by co-injection of Mcad-6 cDNA. CoMO and GFP-myc mRNA-injected embryos showed up to 95% normal eye formation. Statistical significance was confirmed by *t*-test, injections of 200 pg GFP mRNA alone were taken as reference, asterisks indicate *p*-values. $^{*}p < 0.01$, $^{**}p < 0.001$ (C) Eye rescue phenotype: 4 µM Xcad-6MO, 100 pg Mcad-6 cDNA and 200 pg GFP-myc mRNA was injected into one dorsal blastomere of a 4-cell-stage embryo. The successful injection of Xcad-6MO and Mcad-6 was traced by GFP fluorescence (MO+) from outside and further confirmed by myc immunostaining of transverse sections (red fluorescence). White line demarcates the midsagittal plane. Scale bar: 100 µm.

transcripts are already present in early neurula stages, as shown by RT-PCR (stage 12; see David and Wedlich, 2000). Given that in situ hybridization failed to show a transcript localization at this early stage, we dissected the anterior neural plate (ANP) from stage 13 embryos to see by RT-PCR whether Xcadherin-6 is expressed in this region, which consists mostly of the eye field. Indeed, Xcadherin-6 was present exclusively in the ANP and not in the residual mass (Fig. 3A). To verify the correct dissection of the explants, two markers of the early anterior neural plate, Xrx1 and ET1, were included in this RT-PCR. Xrx1 and ET1 also appeared only in the explants, and not in the residual mass. In contrast, β-actin as a control was expressed in the anterior neural plate as well as in the residual embryo. As expected, all transcripts could be amplified in whole embryo RNA extracts.

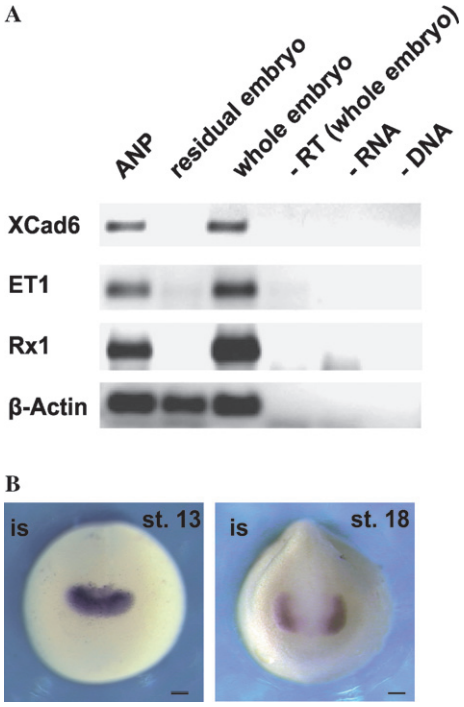

Fig. 3. Xcadherin-6 is expressed in the anterior neural plate but is not required in eye field formation or separation. (A) Gene expression of Xcadherin-6 in stage 13 embryos is restricted to the anterior neural plate (ANP), whereas in the residual embryonic mass no transcript was detected. Correct cutting of the ANP was verified by the presence of the ANP marker genes *ET1* and *Rx1*. The control gene β-actin was expressed in both parts of the embryo as well as in complete embryos. (B) Knockdown of Xcadherin-6 did not influence separation of the eye field as indicated by gene expression of *Rx1* in the early eye field at stages 13 and 18. nis, not injected side; is, injected side. Scale bar: 100 μm.

To investigate a putative role of Xcadherin-6 in eye field separation, Xcad-6MO was injected into one blastomere at two-cell stage. At stage 13 and stage 18, these embryos were subjected to an in situ hybridization with Xrx1. As seen in Fig. 3B, neither eye field formation nor separation was affected by Xcadherin-6 knockdown. We conclude that Xcadherin-6 is expressed in the early eye field, but is not involved in eye field separation.

2.3. Xcadherin-6 is essential for growth of the neural retina and the RPE

To narrow down the time point of eye defects initiated by Xcadherin-6 knockdown, we analyzed single-sided Xcad-6MO-injected embryos from stage 25 to 36 in histological sections. Eye vesicle formation until stage 25 occurred normally and revealed no differences between the injected and the uninjected side of the embryo (Fig. 4A). At the onset of invagination (stage 27) differences in the shape of the outer and inner neuroepithelium of the eye vesicle became obvious. A narrowing of the outer layer and an atypical and irregular thickening of the inner layer were seen on Xcad-6MO-injected sides (Fig. 4B). Immunostaining for aPKC, which marks the apical (ventricular) surface of the inner and outer layer of the optic cup, displayed an atypically folded neuroepithelium in stage 26 embryos (Fig. 4F). Later in development (stages 31, 36), eyes with neural retina, RPE and lenses were found; however, these tissues were smaller in size than in control eyes (Fig. 4C and D). In addition, RPE and neural retina appeared disorganized compared to the control side (Fig. 4E). These morphological defects in eye development were not observed when CoMO was injected (Supplementary Fig. S1).

The reduction in size of the Xcad6-MO eyes suggests that loss of Xcadherin-6 might impede growth or induce cell death in the developing eye. To test for this we performed phosphohistone (PH3) and TUNEL stainings. When PH3-positive nuclei were counted during eye vesicle formation (stage 26), no differences between the injected and the uninjected sides were found (Fig. 5A and B). However, a continuous decrease of mitotic cells was observed in the neural retina and the RPE during eye cup formation (Fig. 5A and B), which temporally correlated with the appearance of the morphological changes in the eye architecture (Fig. 4). Furthermore, the dividing cells appeared dislocated in the retina of the Xcad-6MO-injected side, whereas they were concentrated in the prospective ciliary marginal zone of the uninjected side (data not shown). Apoptotic cells were rarely observed in the developing eye and no significant differences between the Xcad-6MO-injected and uninjected control were found (data not shown). Thus, PH3 and TUNEL staining revealed that the reduced eye size in Xcad-6MO-injected embryos (Figs. 2 and 4) resulted from a decrease in cell divisions rather than from an increase of programmed cell death. The observed defects in eye development, which become visible with eye cup formation correlate with the expression domain of Xcadherin-6. In situ hybridizations reveal a faint signal of ring-like shape when the eye cup is formed (stage 31, Supplementary Fig. S2). With further development the signal fades and becomes restricted to the ciliary marginal zone (stage 34, Supplementary Fig. S2). Taken together, the Xcadherin-6 expression domain and the time point in the appearance of tissue damages in the morphant eye indicate that this cadherin might be required in the morphogenetic movements that give rise to the optic cup before the differentiation of the neuroepithelial layers starts.

2.4. Xcadherin-6 is responsible for proper organization of the neuroepithelium during eye cup formation

In order to elucidate the Xcadherin-6 morpholino effect causing the severe eye defects, we performed transplantation experiments. We co-injected 8 μM Xcadherin-6 or control morpholino (CoMO) together with 200 pg GFP/myc mRNA into the dorsal blastomeres of a four-cell-stage donor embryo (Fig. 6A). A host embryo was injected with 100 pg DsRed2/flag mRNA. By this method, wildtype tissue was labeled with DsRed/flag whereas morpholino-

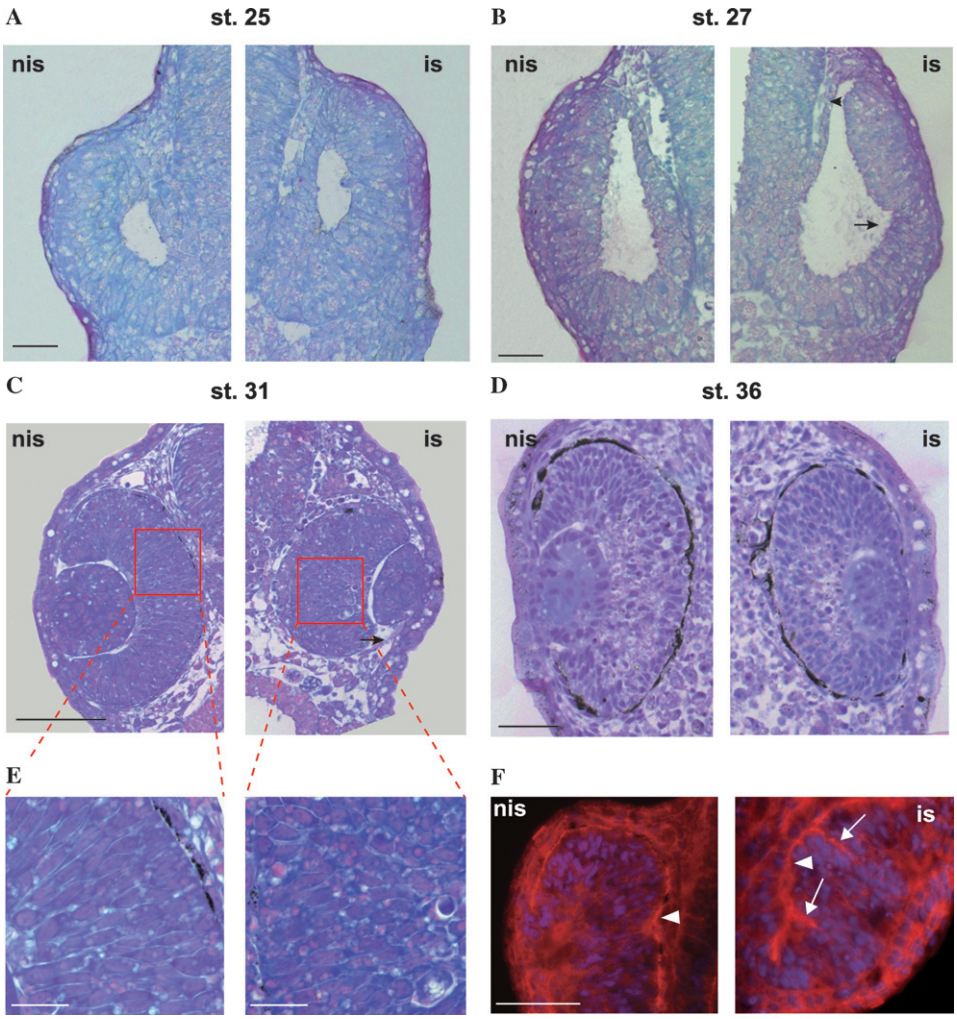

Fig. 4. Organization of the developing retina is disturbed by injection of 8 μM Xcadherin-6 morpholino into one dorsal blastomere of a four-cell-stage embryo. (A) In stage 25 embryos, morphology of inner and outer layers of retina appeared similar between the injected side (is) and the uninjected side (nis). (B) At stage 27, lens induction took place on both sides in a similar fashion. On the injected side, the developing retina shows a narrowing of the prospective RPE (arrowhead) and an artificial thickening in the developing neural retina (arrow). (C) Formation of pigmented retina layer is reduced and laminar structure of the neural retina is disarranged. Eye structure is reduced in size. (D) Organization of the neuroepithelium is disturbed, resulting in a disrupted neural retina and RPE (stage 36). (E) Detail of (C) in higher magnification. (F) Immunostaining for aPKC, labeling the apical surface of the neuroepithelium (arrowheads), reveals a misfolding on the injected side (arrows). In total, 31 embryos were analyzed In stage 25, all 7 embryos were of wildtype morphology. At stage 27, 6 out of 8 embryos exhibited the morpholino phenotype. At stage 31 and 36, 7 out of 8 embryos per stage showed the described phenotype. nis, not injected side; is, injected side. Scale bar: 100 μm, in (E) 20 μm.

containing tissue (Xcad-6MO or CoMO) was marked with GFP/myc. Part of the eye field was transplanted from the donor to the host embryo at stage 13 and the embryo was cultivated until stage 31 (early tadpole). The GFP and DsRed fluorescence served to control the correct position of the grafts and to follow them during eye development from outside. Immunostaining against the myc or flag tag of GFP and DsRed made it possible to study the organization of the eye on sections by confocal microscopy.

The cells of the prospective neural retina and RPE appeared polarized when CoMO-treated eye fields were transplanted into a wildtype environment (Figs. 6C and F; green signal, for orientation see scheme in Fig. 6D). The cells of the inner and outer layer were found highly elongated and tightly packed. In contrast, Xcad-6MO-injected transplants lacked any sign of the typical neuroepithelial organization (Fig. 6B and E). The cells were disordered and less elongated. Disarrangement of cells was observed in the inner (Fig. 6B) and outer layer (Fig. 6E) of Xcadherin-6 depleted graft tissue but not in the directly neighboring host tissue. As listed in Fig. 6J none of the Xcadherin-6 depleted transplants developed a normal optic cup.

We also performed converse transplantations. A transplant from a DsRed2/flag-injected donor was placed into an Xcad-6MO- or CoMO and GFP/myc-injected host (Fig. 6G). The transplanted tissue developed a normal neuroepithelium (Fig. 6H) although the surrounding tissue of the Xcad-6MO-injected host appeared disarranged and

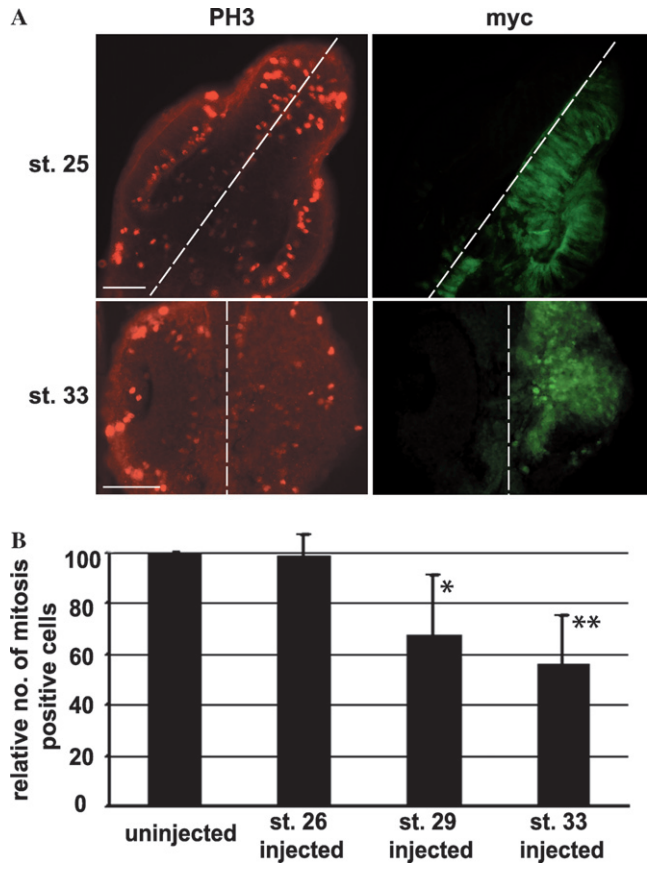

Fig. 5. (A) Xcadherin-6 knockdown led to a decrease in cell proliferation. PH3 staining in a stage 25 embryo injected with Xcad-6MO on one side of the embryo reveals equal numbers of mitosis on injected and uninjected sides of embryo during eye vesicle formation. Myc staining indicates the injected side of the embryo. In stage 33 embryos, the number of mitoses is decreased on the injected side. White line demarcates the midsagittal plane. (B) Statistical analysis of proliferation in Xcadherin-6 depleted eye region. During eye vesicle formation, the number of PH3-positive cells, is nearly identical to that of uninjected embryo sides. During formation of the eye cup, the number of mitoses is continuously decreasing. Ten sections per embryo and 4 embryos per developmental stage were analyzed. PH-3 positive nuclei were counted. The uninjected sides were taken as reference and set to 100%. Statistical significance was confirmed by *t*-test, *p*-values are indicated by asterisks. $^{*}p < 0.01$, $^{**}p < 0.001$. nis, not injected side; is, injected side. Scale bar: 100 μm.

did not display any epithelial organization. Nevertheless, in 55% (10 of 18) normal eye cup development was observed (Fig. 6J). The same experiment with CoMO-injected donor tissue resulted in a well organized neural and pigmented retina structure composed of host and donor cells (Fig. 6I).

2.5. Depletion of Xcadherin-6 disturbs lamination but not cell differentiation in the neural retina

In fully differentiated eyes the destruction of the neural retina and RPE due to Xcad6-MO injections was most prominent. The outer and inner nuclear layers of the neural retina were not properly separated and were disrupted by holes (Fig. 7A, see DAPI staining). Importantly, the lamination of the retinal ganglion cell (RGC) layer took place properly (Fig. 7 arrows, for detailed description of the retina layers see Supplementary Fig. S3), but this layer was reduced in thickness. In bright field images, fragmentation of the RPE was visible (Fig. 7A). Immunostaining for rhodopsin (Fig. 7A) showed that photoreceptor cells were formed, but were delocalized to the nuclear layers where they lined the holes in a rosette like arrangement. Immunostaining for aPKC (Fig. 7B) revealed that the apical surface and the outer segment of the photoreceptor cells were orientated to the centre of these rosettes. Staining for NCAM (Supplementary Fig. S3) confirmed the neuronal fate of the retina cells but also showed the absence of a proper lamination. Lens development was also affected. In situ hybridization revealed a strongly reduced signal for the early lens marker gene *Pitx-3* (Pommereit et al., 2001) at the Xcad6-Mo-injected side (Fig. 8A and B). β1-Integrin immunostaining, which serves as a plasma membrane marker for lens fiber cells (Menko and Philip, 1995) indicated that the lens fiber cells are formed but they are not properly organized in the Xcadherin-6 deficient eye (Fig. 8C–F). Compared to the uninjected eyes the development of the injected ones appeared delayed.

3. Discussion

In this study, we showed by loss-of-function analysis that Xcadherin-6 is essential early in eye development for proper organization and growth of the inner and outer layer of the optic cup. An artificial folding of these layers during invagination and a decrease in proliferation were observed in the absence of Xcadherin-6. Later in development disruption of the RPE, lamination defects in the outer neural retina and a thinner ganglion cell layer were observed. Thus, Xcadherin-6 is required for proper formation and growth of both retina layers, the neural retina and the non-neural RPE.

Cadherin-6 expression in the eye has also been detected in mice (Honjo et al., 2000). The murine cadherin-6 seems to be a functional homologue to Xcadherin-6 as it rescues the knockdown phenotype in *Xenopus* (Fig. 2B). This indicates an evolutionarily conserved role of this cadherin in vertebrate eye development. As functional studies on cadherin-6 in eye development have not been reported so far, our results give the first evidence as to how this cadherin might contribute to the complex adhesion code required in the formation of the visual organ.

First descriptions of cadherin function in *Xenopus* eye development were based on dominant-negative expression studies. They showed defects in eye cup formation and disorganization of the retinal layers for N-cadherin, and fusion of the ventral retina with the floor of the diencephalon for XB-cadherin (Dufour et al., 1994). In the Xcadherin-6 knockdowns we did not observe such phenotypes, which indicate failures in tissue separation. In addition, we demonstrated that separation of the eye field in the anterior neural plate was independent of Xcadherin-6 although Xcadherin-6 transcripts were present at that time.

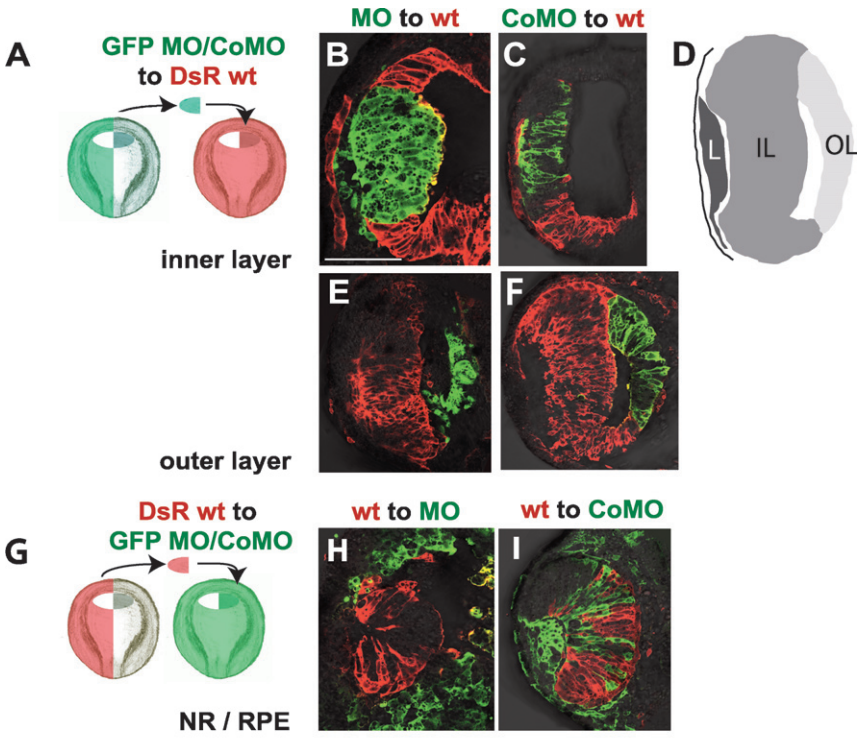

J **Summary of eye field transplantations**

Direction of Transplantation	Number of tranplanted eye fields	Number of normal optic cups at stage 32
Xcad-6MO to wt	14	0
CoMO to wt	4	4
wt to Xcad-6MO	18	10
wt to CoMO	3	2

Fig. 6. Eye field transplantations. (A) Transplants from embryos injected with 8 μM Xcad-6MO or CoMO were inserted into wildtype embryos. As shown in the diagram, grafts were labeled by GFP-myc and the host was labeled with DsRed. (B–F) Transverse sections of eyes containing a graft, immunostained for GFP-myc (green) and DsRed-flag (red). (D) Scheme showing the orientation of the eyes in the sections. (B, E) Xcad-6MO transplants (green) embedded in inner (B) or outer layer (E) show aberrant neuroepithelial organization. (C, F) CoMO transplants (green) integrated into inner (C) or outer layer (F) exhibit proper organization. (G) Transplants from wildtype embryos were inserted into embryos injected with 8 μM Xcad-6MO or CoMO. As shown in the diagram, grafts were labeled with DsRed-flag and the host was labeled with GFP-myc. (H, I) Transverse sections of eyes containing a graft, immunostained for GFP-myc (green) and DsRed-flag (red). (H) The DsRed-labeled eye field gives rise to a normal retina structure (red) in an Xcad-6MO host environment (green). (I) Wildtype graft (red) in CoMO-injected host (green) develop a normal retina consisting of donor and host tissue. (J) Table summarizing the outcome of all transplantations. None of the Xcad-6MO containing transplants led to normal eye cup formation whereas 10 of 18 wildtype grafts developed a normal eye cup in a Xcad-6 depleted tissue surrounding. CoMO containing transplants developed properly. In converse transplantations one graft failed to develop an optic cup. L, lens; IL, inner layer; OL, outer layer. Scale bar: 100 μm.

However; we also observed disarranged retina layers in Xcadherin-6 deficient embryos. Different kinds of disarrangements ranging from clumping of photoreceptor cells in protocadherin-15b deficient zebrafish (Seiler et al., 2005) to complete loss of neural retina lamination in the N-cadherin zebrafish mutant *parachute* (Masai et al., 2003) have been reported. With regards to these loss-of-function phenotypes cadherins have been put into two main functional classes; establishment of neuroepithelial polarity and retina differentiation. We assign Xcadherin-6 more to the group involved in stabilizing neuroepithelial polarity rather than retina differentiation. The latter was affected in R-cadherin (Cdh4) knockdowns because loss of photoreceptor cells and reduced expression of the differentiation markers *crx* and *otx* were observed (Babb et al., 2005). In Xcadherin-6 deficient embryos with abnormal eyes photoreceptor cells were always present, making an involvement of this cadherin in photoreceptor cell differentiation most unlikely. However, photoreceptor cells arranged in rosettes were found mislocated in the outer retina, indicating a loss of neuroepithelial polarity as described for the N-cadherin knockout phenotype but to a less severe degree. Studies of two *N-cadherin* (*cdh2*) mutants, *parachute* and *glass onion,* and cdh2 antisense

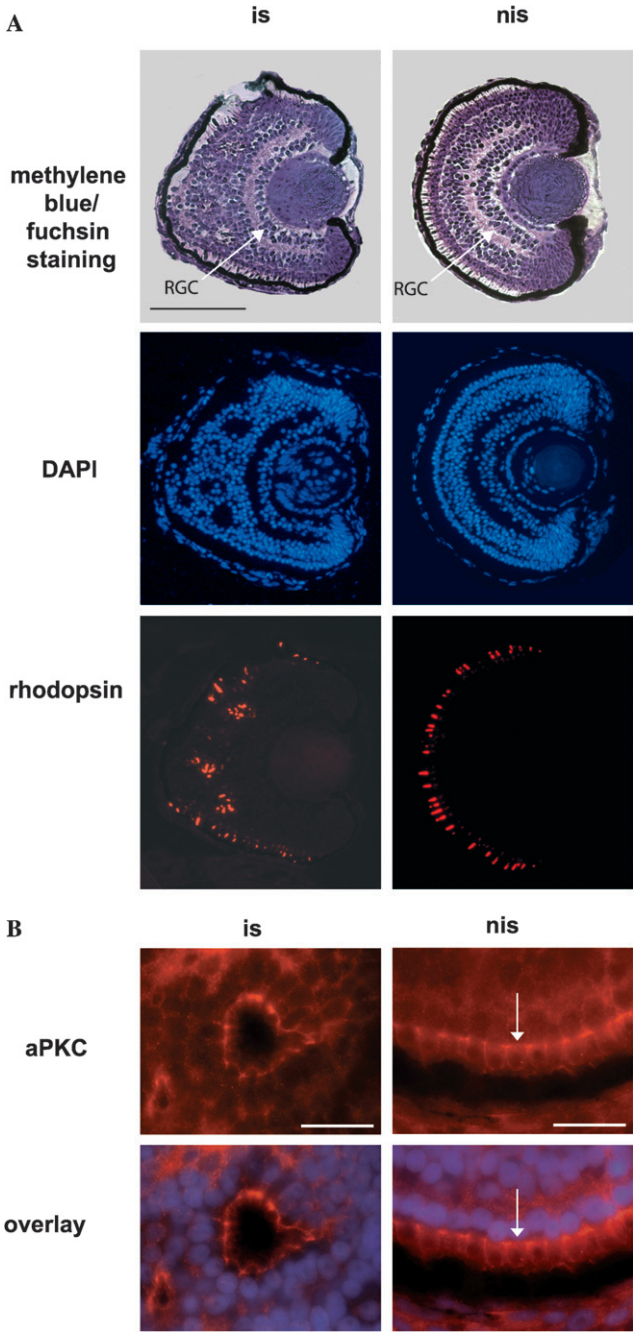

Fig. 7. Phenotype of fully differentiated eyes of stage 46 embryos. (A) Histological staining of eyes reveals a strongly disorganized neural retina and fragmentaton of the retina pigment epithelium on the injected side. DAPI images of the corresponding eyes demonstrate destroyed morphology of outer and inner nuclear layers. Immunostaining for rhodopsin reveals differentiated sensory cells. In the injected eyes rosette structures form, misplaced in the INL. Arrow points to retina ganglion cell layer (RGC). (B) The rosette structures consist of polarized photoreceptor cells. The apical side is stained by aPKC, the basal side has nuclear staining with DAPI in the overlay. On the non-injected side the correct organization of photoreceptor cells is displayed by the aPKC staining of the outer limiting membrane (arrows). In injected eyes photoreceptors are localized around the rosettes with the apical side pointing towards the centre. nis, not injected side; is, injected side. Scale bars: in (A): 100 μm, in (B): 25 μm.

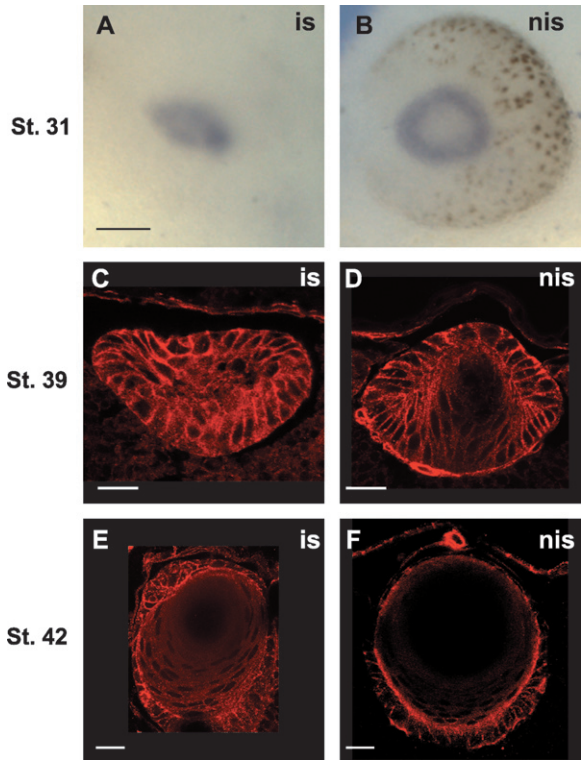

Fig. 8. Depletion of Xcadherin-6 disturbs lens development. (A) In situ hybridization of Xcadherin-6 depleted embryos demonstrates a reduction in the expression of the lens marker gene *Pitx-3* on the injected side in stage 31 embryos. (C–F) Staining for β1-integrin shows the organization of lens fiber cells. On the injected side the cells are not properly arranged. nis, not injected side; is, injected side. Scale bars in (A, B): 50 μm, in (C–F): 10 μm.

morpholino knockdown revealed severe lamination defects. All neural retina layers were affected. They were partially fused and showed disruptions of the IPL (Erdmann et al., 2003; Malicki et al., 2003; Masai et al., 2003). Importantly, neuroepithelial polarity was lost, as was visible by the displacement of the centrosomes from the apical surface in the ventral retina (Malicki et al., 2003; Masai et al., 2003). We used the apical aPKC as marker for neuroepithelial polarity. This protein was found localized at the apical surface of frog blastomeres (Chalmers et al., 2003). During normal eye development we detected aPKC at the apical surface of the outer and inner layer of the invaginating neuroepithelium. With neurogenesis aPKC was localized in the outer limiting membrane of the neural retina and, in the photoreceptor cells between their outer and inner segment. In the photoreceptor rosettes the outer segments and the apical membranes pointed to the centre while the basally localized nuclei were in the outer circle. Thus, cell polarity of the photoreceptor cell was unaffected as described for zebrafish glass onion mutants (Pujic and Malicki, 2001). However, the neuroepithelial integrity was abolished in *parachute (pac)* and glass onion mutants. Cells form rosettes mostly filled with morphologically indistinct cells or plexiform layer tissue dis-

turbing the inner nuclear layer, the retinal ganglion layer and the photoreceptor cell layer (Erdmann et al., 2003; Masai et al., 2003). In the Xcadherin-6 morphants rosettes are only formed by photoreceptor cells and restricted to the outer retina. Therefore, we assume that the mechanisms leading to the lamination defects observed in Xcadherin-6 morphants are different from those found in N-cadherin mutants. Xcadherin-6 knockdown results selectively in atypical folding of the invaginating neuroepithelium as seen in histological sections and by aPKC localization. At this period the polarity of the prospective retina and RPE was maintained as aPKC was found at the ventricular surface of the optic cup. However, histological sections and transplantations revealed that cells appeared less elongated and disorganized in the neuroepithelium. Thus, Xcadherin-6 is required for proper organization of the neuroepithelium in the primordia of neural retina and RPE before their differentiation starts. We suggest that the later observed fragmentation of the RPE and the rosette formation of the photoreceptor cells are caused by ligations of atypically folded inner and outer layers of the optic cup. A weakness of cell adhesion in Xcadherin-6 knockdowns might facilitate incorrect folding of these layers.

Apart from lamination defects in the neural retina and fragmentation of the RPE the size of the eye was reduced. Different to FAT1$^{-/-}$ mice (Ciani et al., 2003) and to R-cadherin knockdown in zebrafish (Babb et al., 2005), we observed no dramatic increase in apoptosis. Instead, proliferation was reduced with the onset of neurogenesis. Therefore, the small eye phenotype in *Xenopus* is explained by growth reduction and not degeneration via apoptosis as is the case in FAT1$^{-/-}$ mice and R-cadherin deficiency in zebrafish.

Lens development was also affected by Xcadherin-6 knockdown. Lenses were smaller and fiber cells were found disarranged and developmentally delayed. A quite similar phenotype was found in the zebrafish N-cadherin mutant *parachute* (Masai et al., 2003). We presume that the misfolding neuroepithelium impairs lens development as a secondary effect.

In summary, we demonstrated that Xcadherin-6 is crucial for growth and epithelial development of both retina layers, the RPE and the neural retina. Our results show the beginning of the invagination at stage 27 as the main target of Xcadherin-6 function. Changes in morphology as well as in rate of mitosis occurred during or near this important phase of morphogenetic movement in the absence of Xcadherin-6. The later defects in lamination might be a consequence of this early requirement.

4. Experimental procedures

4.1. Histological procedures and immunostaining

Embryos were staged according to Nieuwkoop and Faber (1967). They were fixed in 3.7% formaldehyde in MEM (0.1 M MOPS, 2 mM EGTA, and 1 mM $MgSO_4$) for 2 h at RT. For vibratome sections, embryos were embedded in 3% agarose in APBS/Ca^{2+} (amphibian phosphate-buffered saline, 2.7 mM KCl, 0.15 mM KH_2PO_4, 103 mM NaCl, 0.7 mM Na_2HPO_4, and 2 mM $CaCl_2$, pH 7.5) and transversely cut into 50 μm- sections. Cryosections were prepared as previously described (Fagotto and Gumbiner, 1994).

For immunostaining, sections were blocked with 1% BSA + 1% fetal calf serum (FCS) in 1x APBS for 1 h at RT before incubation with primary antibody in blocking solution overnight at 4 °C. Sections were then washed with APBS/0.1% Tween 20 and APBS/Tween 20 with 0.3 M NaCl and incubated with the corresponding secondary antibody for 2 h. After washing, the sections were mounted, embedded in elvanol and analyzed by fluorescence microscopy (DMIRE2, Leica, Benzheim, Germany) or laser confocal microscopy (TCS40, Leica, Solms, Germany).

The following antibody combinations were used: 1/400 rabbit polyclonal flag antibody (Sigma, Deisenhofen, Germany), 1/200 rabbit phosphohistone H3 antibody (Upstate, Charlottesville, USA), 1/200 rabbit polyclonal aPKC (Santa Cruz, nPKCζ (C-20) sc-216), 1/50 mouse monoclonal β1-integrin (Gawantka et al., 1992), 1/100 mouse monoclonal Rhodopsin, 1/200 mouse monoclonal NCAM, and mouse monoclonal 9E10 myc undiluted cell culture supernatant. As secondary antibodies we used goat-anti-mouse or goat–anti-rabbit conjugated to Cy2 or Cy3 in 1/400 dilution (Dianova, Hamburg, Germany).

Histological staining was performed on Technovit-embedded sections. Fixed embryos were infiltrated with Technovit for 24 h and then transferred into the embedding solution. Five-micrometer-thick sections were cut on a microtome and dried over night at 37 °C. For staining, sections were dipped briefly in methylene blue/basic fuchsin and cleared in 95% alcohol before being embedded in DePeX (Serva, Heidelberg, Germany).

4.2. Injections and transplantations

The Xcadherin-6 morpholino as well as the control morpholino oligonucleotides were designed and synthesized by GeneTools (Philomath, OR, USA). Fertilized *Xenopus laevis* eggs were cultured and microinjected as described previously (Geis et al., 1998). Morpholino oligonucleotides (Xcad-6MO and CoMO) were applied at concentrations of 4 or 8 μM in 4 nl volume, respectively in one blastomere at the two-cell stage or in one dorsal blastomere at the 4-cell stage. Concentrations of 8 μM morpholinos were preferentially used to increase the frequency in phenotype for transplantations and histological analyses. As an injection control, 200 pg GFP/myc mRNA was co-injected. The rescue construct of mouse Cadherin-6 in pCA-pA vector was obtained from Takayoshi Inoue, Kansas City, USA. For rescue experiments, 100 pg of this cDNA was co-injected into the fertilized eggs.

Transplantation of the eye field of *X. laevis* embryos was carried out as previously described for cranial crest cells (Borchers et al., 2000) with some modifications. The donor embryos were injected with either a combination of 8 μM Xcadherin-6 morpholino oligonucleotide and 200 pg GFP/myc mRNA or 400 pg DsRed2/flag into two dorsal blastomeres of 4-cell stage embryos, whereas the host embryos were prepared by co-injection of 8 μM Xcadherin-6 morpholino oligonucleotide and 200 pg GFP/myc mRNA or 400 pg DsRed2/flag into two dorsal blastomeres of 4-cell stage embryos. The DsRed2/flag construct was created by PCR amplification of the 680 bp DsRed2 insert from the DsRed2-N1 plasmid (Clontech, Palo Alto, CA, USA) Primer sequences were: EcoRI_5′ CAAGAATTCCATG GCCTCCTCC, XhoI_3′ GAACTCGAGCTACAGGAACAGGTG. The amplificate was cloned into a pCS2/flag vector. Eye fields were removed from the anterior neural plate of stage 13 donor embryos according to the expression area of the early eye marker Xrx (Ohnuma et al., 2002). Host embryos were prepared accordingly, and the transplant of eye field was placed in the corresponding cavity of the host. Following documentation of the graft with a microscope (MZFL III, Leica, Benzheim, Germany) the embryos were fixed for histological analysis.

4.3. RT-PCR

The anterior neural plate in each of 20 stage 12 *X. laevis* embryos was explanted and collected. RNA was extracted from this part as well as from the residual embryo and from 20 whole embryos (SV Total RNA Isolation

Kit, Promega, Mannheim, Germany). For analysis of eye explants, 59 eyes of stage 26 embryos as well as 70 eyes of stage 44 embryos were extracted. One microgram total RNA was reverse transcribed (ImProm-II Reverse Transcription Kit, Promega) and 4 μl cDNA was amplified by standard PCR procedures. The primers used were:

Xcad-6: 5′: AGTCTTCCCCTGTGGGTTCT;
3′: CTGGGCCAAAACTGTTCCTA
ET1: 5′: CCTATCCTTGACTTGCTACA;
3′: GTTTTGGGGAAGGAGGGTAT
Rx1: 5′: CCCCAACAGGAGCATTTAGAAGAC;
3′: AGGGCACTCATGGCAGAAGGTT
β-actin: 5′: GCGTACCTCATGAAGATCCT;
3′: GCGGATGTCCACGTCACACT

4.4. In situ hybridization

Morpholino-injected embryos of different stages were fixed in MEM-FA for 1 h and stored in ethanol at −20 °C. In situ hybridizations were carried out as described earlier (Hollemann et al., 1998). The Rx1 plasmid was linearized with *Bam*HI, the Pitx-3 plasmid with *Not*I, and both were transcribed in vitro with T7 for antisense probes and DIG-labeled nucleotides (Roche, Mannheim, Germany). The embryos were analyzed under a microscope (MZFL III, Leica). The Xcadherin-6 probe was prepared as described in David and Wedlich (2000).

4.5. Antibody generation and immunoblotting

A rabbit polyclonal antibody was raised against the peptide H2N-FFL LEE YTG SDY QYC-CONH2 (EC1-1) covering part of the EC1 domain of Xcadherin-6 (Eurogentec, Seraing, Belgium). The antiserum was purified by a two-step protocol of a protein A and a peptide-specific NHS affinity column (Pharmacia, Freiburg, Germany). The specificity of the purified Xcadherin-6 antibody was tested using in vitro translated fusion proteins with GFP or myc tag: full-length Xcadherin-6/GFP in pCDNA 3.1/CT-GFP, full-length Xcad-11/myc in pCDNA 3.1/Myc-His, full-length XE-cadherin/myc in pBSK+. The fusion proteins were synthesized in vitro using the transcription and translation kit (TNT) from Promega (Mannheim, Germany) according to the manufacturer's instructions. For immunoblot of embryo lysates 20 injected or uninjected embryos of desired stage were lysed in 200 μl NOP buffer (150 mM NaCl, 10 mM Tris/HCl, 1 mM $MgCl_2$, 0.75 mM $CaCl_2$, and 2% Nonidet P40, pH 7.8). The NOP lysate was mixed with concanavalin A (Con A)-coupled Sepharose (Sigma) suspension. The lysates were incubated for 90 min at 4 °C. After centrifugation the pellet was resuspended in SDS–PAGE sample buffer and boiled. For immunoblotting, 5 μl of the in vitro TNT lysates or an equivalent of 5 embryos per slot were loaded on SDS–PAGE. After blotting to a nitrocellulose membrane, the filter was incubated with primary antibody overnight at 4 °C using the rabbit polyclonal Xcadherin-6 antibody, the mouse monoclonal XE-cadherin antibody, the affinity purified mouse monoclonal 9E10 myc antibody and the mouse monoclonal GFP antibody. After incubation for 2 h at room temperature (RT) with the corresponding horseradish peroxidase-conjugated secondary antibodies (Dianova, Hamburg, Germany), the immunoreactive proteins were visualized using the enhanced *ECL*™ Western blotting detection system (Amersham, Braunschweig, Germany).

Acknowledgements

We thank Robert Vignali, University of Pisa, for providing the Rx1 clone, Takayoshi Inoue, Stowers Institute, Kansas City, for the Mcad-6 construct; and Paul Hargrave, University of Florida, Gainsville, for the Rhodopsin antibody. Thomas Hollemann, University of Halle, and Tomas Pieler, University of Goettingen, kindly provided the Pitx-3 probe. We also thank Christine van Lishout for technical assistance. The work was supported by the German Research Foundation (DFG, We 1208/9).

Appendix A. Supplementary data

Supplementary data associated with this article can be found, in the online version, at doi:10.1016/j.mod.2006.08.010.

References

Angst, B.D., Marcozzi, C., Magee, A.I., 2001. The cadherin superfamily: diversity in form and function. J. Cell Sci. 114, 629–641.
Babb, S.G., Kotradi, S.M., Shah, B., Chiappini-Williamson, C., Bell, L.N., Schmeiser, G., Chen, E., Liu, Q., Marrs, J.A., 2005. Zebrafish R-cadherin (Cdh4) controls visual system development and differentiation. Dev. Dyn. 233, 930–945.
Bekirov, I.H., Needleman, L.A., Zhang, W., Benson, D.L., 2002. Identification and localization of multiple classic cadherins in developing rat limbic system. Neuroscience 115, 213–227.
Borchers, A., Epperlein, H.H., Wedlich, D., 2000. An assay system to study migratory behavior of cranial neural crest cells in *Xenopus*. Dev. Genes Evolut. 210, 217–222.
Bron, A.J., Tripathi, R.C., Tripathi, B.J., 1997. Wolff's Anatomy of the Eye & Orbit. Chapman & Hall, London.
Chalmers, A.D., Strauss, B., Papalopulu, N., 2003. Oriented cell divisions asymmetrically segregate aPKC and generate cell fate diversity in the early *Xenopus* embryo. Development 130, 2657–2668.
Ciani, L., Patel, A., Allen, N.D., ffrench-Constant, C., 2003. Mice lacking the giant protocadherin mFAT1 exhibit renal slit junction abnormalities and a partially penetrant cyclopia and anophthalmia phenotype. Mol. Cell. Biol. 23, 3575–3582.
David, R., Wedlich, D., 2000. *Xenopus* cadherin-6 is expressed in the central and peripheral nervous system and in neurogenic placodes. Mech. Dev. 97, 187–190.
Dufour, S., Saint-Jeannet, J.P., Broders, F., Wedlich, D., Thiery, J.P., 1994. Differential perturbations in the morphogenesis of anterior structures induced by overexpression of truncated XB- and N-cadherins in *Xenopus* embryos. J. Cell Biol. 127, 521–535.
Erdmann, B., Kirsch, F.P., Rathjen, F.G., More, M.I., 2003. N-cadherin is essential for retinal lamination in the zebrafish. Dev. Dyn. 226, 570–577.
Fagotto, F., Gumbiner, B.M., 1994. Beta-catenin localization during *Xenopus* embryogenesis: accumulation at tissue and somite boundaries. Development 120, 3667–3679.
Gawantka, V., Ellinger-Ziegelbauer, H., Hausen, P., 1992. Beta 1-integrin is a maternal protein that is inserted into all newly formed plasma membranes during early *Xenopus* embryogenesis. Development 115, 595–605.
Geis, K., Aberle, H., Kuhl, M., Kemler, R., Wedlich, D., 1998. Expression of the Armadillo family member p120cas1B in *Xenopus* embryos affects head differentiation but not axis formation. Dev. Genes Evol. 207, 471–481.
Hatta, K., Takeichi, M., 1986. Expression of N-cadherin adhesion molecules associated with early morphogenetic events in chick development. Nature 320, 447–449.
Hoar, R.M., 1982. Embryology of the eye. Environ. Health Perspect. 44, 31–34.
Hollemann, T., Bellefroid, E., Pieler, T., 1998. The *Xenopus* homologue of the Drosophila gene tailless has a function in early eye development. Development 125, 2425–2432.
Honjo, M., Tanihara, H., Suzuki, S., Tanaka, T., Honda, Y., Takeichi, M., 2000. Differential expression of cadherin adhesion receptors in

neural retina of the postnatal mouse. Invest. Ophthalmol. Vis. Sci. 41, 546–551.

Inoue, T., Tanaka, T., Takeichi, M., Chisaka, O., Nakamura, S., Osumi, N., 2001. Role of cadherins in maintaining the compartment boundary between the cortex and striatum during development. Development 128, 561–569.

Kemler, R., 1992. Classical cadherins. Semin. Cell Biol. 3, 149–155.

Li, H., Tierney, C., Wen, L., Wu, J.Y., Rao, Y., 1997. A single morphogenetic field gives rise to two retina primordia under the influence of the prechordal plate. Development 124, 603–615.

Liu, Q., Sanborn, K.L., Cobb, N., Raymond, P.A., Marrs, J.A., 1999. R-cadherin expression in the developing and adult zebrafish visual system. J. Comp. Neurol. 410, 303–319.

Liu, Q., Babb, S.G., Novince, Z.M., Doedens, A.L., Marrs, J., Raymond, P.A., 2001. Differential expression of cadherin-2 and cadherin-4 in the developing and adult zebrafish visual system. Vis. Neurosci. 18, 923–933.

Malicki, J., Jo, H., Pujic, Z., 2003. Zebrafish N-cadherin, encoded by the glass onion locus, plays an essential role in retinal patterning. Dev. Biol. 259, 95–108.

Masai, I., Lele, Z., Yamaguchi, M., Komori, A., Nakata, A., Nishiwaki, Y., Wada, H., Tanaka, H., Nojima, Y., Hammerschmidt, M., Wilson, S.W., Okamoto, H., 2003. N-cadherin mediates retinal lamination, maintenance of forebrain compartments and patterning of retinal neurites. Development 130, 2479–2494.

Matsunaga, M., Hatta, K., Takeichi, M., 1988. Role of N-cadherin cell adhesion molecules in the histogenesis of neural retina. Neuron 1, 289–295.

McNeill, H., Ozawa, M., Kemler, R., Nelson, W.J., 1990. Novel function of the cell adhesion molecule uvomorulin as an inducer of cell surface polarity. Cell 62, 309–316.

Menko, A.S., Philip, N.J., 1995. Beta 1 integrins in epithelial tissues: a unique distribution in the lens. Exp. Cell Res. 218, 516–521.

Nelson, W.J., Hammerton, R.W., Wang, A.Z., Shore, E.M., 1990. Involvement of the membrane-cytoskeleton in development of epithelial cell polarity. Semin. Cell Biol. 1, 359–371.

Nieuwkoop, P.D., Faber, J., 1967. Normal Table of *Xenopus laevis* (Daudin). Elsevier North-Holland Biomedical Press, Amsterdam.

Nollet, F., Kools, P., van Roy, F., 2000. Phylogenetic analysis of the cadherin superfamily allows identification of six major subfamilies besides several solitary members. J. Mol. Biol. 299, 551–572.

Ohnuma, S., Mann, F., Boy, S., Perron, M., Harris, W.A., 2002. Lipofection strategy for the study of *Xenopus* retinal development. Methods 28, 411–419.

Patel, S.D., Ciatto, C., Chen, C.P., Bahna, F., Rajebhosale, M., Arkus, N., Schieren, I., Jessell, T.M., Honig, B., Price, S.R., Shapiro, L., 2006. Type II cadherin ectodomain structures: implications for classical cadherin specificity. Cell 124, 1255–1268.

Pommereit, D., Pieler, T., Hollemann, T., 2001. Pitx3: a member of the Rieg/Pitx gene family expressed during pituitary and lens formation in *Xenopus laevis*. Mech. Dev. 102, 255–257.

Pujic, Z., Malicki, J., 2001. Mutation of the zebrafish glass onion locus causes early cell-nonautonomous loss of neuroepithelial integrity followed by severe neuronal patterning defects in the retina. Dev. Biol. 234, 454–469.

Redies, C., Takeichi, M., 1996. Cadherins in the developing central nervous system: an adhesive code for segmental and functional subdivisions. Dev. Biol. 180, 413–423.

Seiler, C., Finger-Baier, K.C., Rinner, O., Makhankov, Y.V., Schwarz, H., Neuhauss, S.C., Nicolson, T., 2005. Duplicated genes with split functions: independent roles of protocadherin15 orthologues in zebrafish hearing and vision. Development 132, 615–623.

Shapiro, L., Fannon, A.M., Kwong, P.D., Thompson, A., Lehmann, M.S., Grübel, G., Legrand, J.F., Als-Nielsen, J., Colman, D.R., Hendrickson, W.A., 1995. Structural basis of cell–cell adhesion by cadherins. Nature 374, 327–337.

Shimoyama, Y., Tsujimoto, G., Kitajima, M., Natori, M., 2000. Identification of three human type-II classic cadherins and frequent heterophilic interactions between different subclasses of type-II classic cadherins. Biochem. J. 349, 159–167.

Takeichi, M., 1995. Morphogenetic roles of classic cadherins. Curr. Opin. Cell Biol. 7, 619–627.

Tanabe, K., Takeichi, M., Nakagawa, S., 2004. Identification of a nonchordate-type classic cadherin in vertebrates: chicken Hz-cadherin is expressed in horizontal cells of the neural retina and contains a nonchordate-specific domain complex. Dev. Dyn. 229, 899–906.

Wöhrn, J.-C., Puelles, L., Nakagawa, S., Takeichi, M., Redies, C., 1998. Cadherin expression and retinofugal pathways of the chicken embryo. J. Comp. Neurol. 396, 20–38.

Woo, K., Fraser, S.E., 1995. Order and coherence in the fate map of the zebrafish nervous system. Development 121, 2595–2609.

Xu, L., Overbeek, P.A., Reneker, L.W., 2002. Systematic analysis of E-, N- and P-cadherin expression in mouse eye development. Exp. Eye Res. 74, 753–760.

Yagi, T., Takeichi, M., 2000. Cadherin superfamily genes: functions, genomic organization, and neurologic diversity. Genes Dev. 14, 1169–1180.